京都大学防災研究所年報 第 49 号 B 平成 18 年 4 月
Annuals of Disas. Prev. Res. Inst., Kyoto Univ., No. 49 B, 2006

Experimental and Numerical Study on Migration of LNAPL under the Influence of Fluctuating Water Table in Subsurface

Masashi KAMON*, Yan LI*, Giancarlo FLORES**, Toru INUI* and Takeshi KATSUMI*

* Graduate School of Global Environmental Studies, Kyoto University
** Sun Yat-sen University, China
*** Graduate School of Engineering, Kyoto University

Synopsis

In this study, the results of *NAPL Simulator* which is used to predict the behavior of benzene (an LNAPL) under fluctuating groundwater table conditions are analyzed. A very good correlation was found between water saturation, capillary pressure and the location of the water table, and it was confirmed that the hysteresis phenomenon makes the *S-p* relations history and path dependant. A slightly modified *NAPL Simulator* code made a good prediction of water saturation, water flow, LNAPL flow, water table and LNAPL table of the column test. The modified version was then used to simulate the behavior of benzene at a contaminated subsurface under the influence of groundwater table fluctuation and the results were compared to the actual in-situ investigated results. Both the simulation and the actual investigated results showed a great correspondence, demonstrating that the modified *NAPL Simulator* code predicts accurately the behavior of benzene under fluctuating water table conditions.

Keywords: groundwater, contamination, benzene, LNAPL, column test, *S-p* relation

1. Introduction

By definition, *Non-Aqueous Phase Liquids* (NAPLs) are the liquids that are not readily miscible with water and air. NAPLs are further classified as *Light Non-Aqueous Phase Liquids* (LNAPLs) when their densities are lower than water, and as *Dense Non-Aqueous Phase Liquids* (DNAPLs) when their densities are greater than water.

When a small amount of LNAPL is released into the subsurface, it will migrate through the unsaturated zone until it distributes itself as a residual saturation. If the release is large enough, it will reach the capillary fringe where it will spread laterally above the saturated zone.

To effectively select and design appropriate remedial programs for these spills, we must consider groundwater table fluctuations. For instance, when the water table is lowered, the mobile LNAPL will also migrate downward re-establishing itself above the new water table location. If the water table is subsequently raised, LNAPL will rise and re-establish itself on top of the water table under imbibition conditions, and a portion of the LNAPL will remain trapped in the saturated region. The trapped fraction will increase the volume of LNAPL that can be partitioned to the aqueous phase and be carried off site as result of groundwater flow in the saturated zone.

In this paper, three features will be focused. The first one will be the characterization of the mechanism of LNAPL migration under fluctuating water table conditions via a column test experiment to measure the *S-p* relationship. The second one will be the simulation of the characteristics of LNAPL migration on the mentioned column test using *NAPL Simulator* (Guarnaccia et al. 1997). Finally, the modified NAPL

Simulator code will be employed to simulate the characteristics of an in-situ benzene-contaminated subsurface under the influence of water table fluctuation.

2. Experimental Study

2.1 Experimental Apparatus

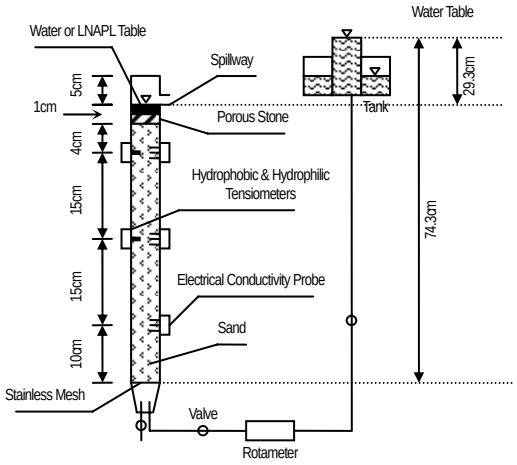

Fig. 1 Apparatus for the column test

Figure 1 shows the schematic system used for the measurement of *S-p* relations in an LNAPL-water porous medium under fluctuating water table. An acrylic column (3.5 cm inner diameter, 4.5 cm external diameter, 50 cm length) with two pairs of tensiometers assembled along one side, and three electrical conductivity probes assembled on the opposite side, was filled with fully saturated Toyoura sand. Each pair of tensiometers is composed of one hydrophobic and one hydrophilic tensiometer, which measure pore LNAPL pressure and pore water pressure respectively. The electrical conductivity probes are used to estimate water saturation via the measurement of the soil system electrical conductivity. The design and preparation of this system was covered by Endo (2002) and Kamon et al. (2003).

2.2 Materials

Toyoura sand with soil particle density of 2.64 g/cm^3, compacted state void ratio of 0.62, saturated density of 2.01 g/cm^3, and grain size distribution as shown in Fig. 2, was used as the sandy porous medium

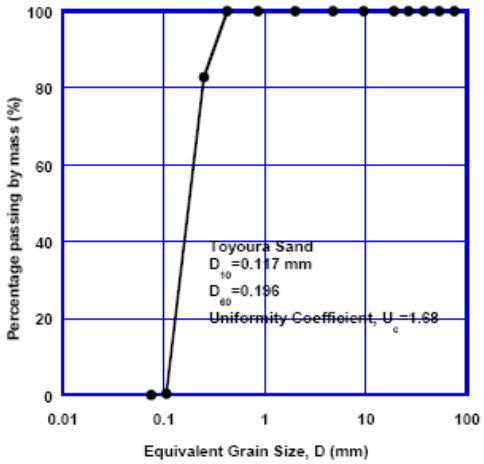

Fig. 2 Toyoura sand grain size distribution

A sodium chloride solution with a concentration of 0.05 mol/L was used as initial pore liquid in order to raise reactivity of the electrical conductivity probe, and to avoid the formation of condenser component in the soil system (Kamon et al. 2003). The saturation of sandy medium was achieved by underwater falling method. After pouring 0.05 mol/L salt water in a volume

Table 1 Properties of the materials

	Liquid Paraffin	Sudan III	Water
Formula		$C_{22}H_{16}N_4O$	H_2O
Appearance	Colorless, odorless	Red powder	Colorless, odorless
Boiling Point	>300°C		100°C
Melting Point	<-10°C	100°C	0°C
Evaporation Rate	Non volatile		
Solubility	Insoluble in water	Water solubility < 0.1g/l	
Viscosity	170 mpa·s		
Hazard Nature	Non toxic		
Surface Tension	31.07 mN/m (25°C)		72.75 mN/m
Interfacial Tension	62.06 mN/m (25°C)		
Specific Gravity	0.87 g/cm^3		0.998 g/cm^3

equivalent to two pore volume of the sand sample into the column, the sand sample was also poured layer by layer, uniformly, using a funnel. Simultaneously, pore water was extracted from the bottom of the column and corresponding volume of the same salt water was filled into the sand medium from the top of the column. Thus, before drainage process began, the sandy medium had been fully saturated with salt water.

Liquid paraffin was used as a LNAPL due to its very low volatility at room temperature, negligible solubility in water and safety of use. LNAPL was dyed with Sudan III with a weight ratio of 10000:1. The properties of these materials are shown in Table 1.

2.3 Column Test

The column test can be described as having two sequential cycles with four successive parts: the first descent (or drainage) of the water table, the first ascent (or imbibition), the second descent and the second ascent. The whole process is characterized by the position of the water tank, as shown in Fig. 3.

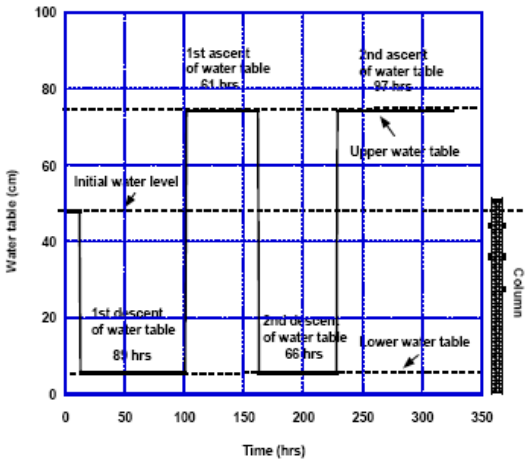

Fig. 3 Variation of the water tank position

(1) Initial condition

The Toyoura sand in the column was fully saturated with 0.05 mol/L salt water. The height of the column water table was 45 cm above the bottom of the column.

(2) First descent of the water table

The water tank was lowered from 45 cm to 5.5 cm above the bottom of the column. As the column water table went down accordingly, pore water flowed out from the bottom of the column due to gravity. Simultaneously, the same volume of LNAPL was automatically infiltrated into the sand from the top of the column. During this process, LNAPL displaced the pore water in the sand. Thus, the process can be regarded as a natural incomplete drainage process during which a 1 cm LNAPL layer existed all the time over the sand. This process took 89 hours.

(3) First ascent of the water table

After the first descent process of the water table finished, the water tank was moved up from 5.5 cm to 74.3 cm above the bottom of the column. As the column water table moved up due to the upward water pressure, LNAPL was pushed up and displaced by water and flowed out of the column from the spillway on top of it. The same volume of water was also automatically infiltrated into the porous medium from the bottom of the column. This process can be regarded as a natural incomplete imbibition process. Again, there was a 1 cm liquid layer over the sand at all times. This process took 61 hours.

(4) Second descent of the water table

After the first ascent process of the water table finished, the water tank was brought down again from 74.3 cm to 5.5 cm above the bottom of the column. LNAPL displaced the pore water in the sand medium, and the pore water was driven out of the column due to gravity. During this process a 1 cm LNAPL layer existed over the sand at all times. This process took 66 hours.

(5) Second ascent of the water table

After the second descent process of the water table finished, the water tank was moved up again from 5.5 cm to 74.3 cm above the bottom of the column. LNAPL was displaced by the water infiltrated from the bottom of the column, and the pore LNAPL was driven out of the column via the spillway. At all times a 1cm liquid layer was present over the sand. This process took 97 hours.

(6) Results of the Column Test

Saturation and capillary pressure values over time are shown in Fig. 4. It is evident from the graphic that when the water table fell, the water saturation of the sand decreased and the capillary pressure increased and, when the water table raised, the water saturation increased and the capillary pressure decreased accordingly. There is a good correspondence between water saturation, capillary pressure and the water table. In Figure 4, the first

drainage process occurred from hour 0 to 89, the first imbibition process from hour 89 to 162, the second drainage process from hour 162 to 228, and the second imbibition process from hour 228 to 325.

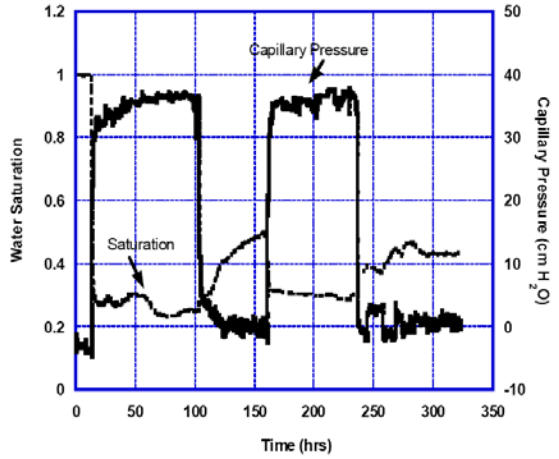

Fig. 4. Water saturation and capillary pressure during the column test

The water saturation - capillary pressure (*S-p*) relation during the test is shown in Fig 5.

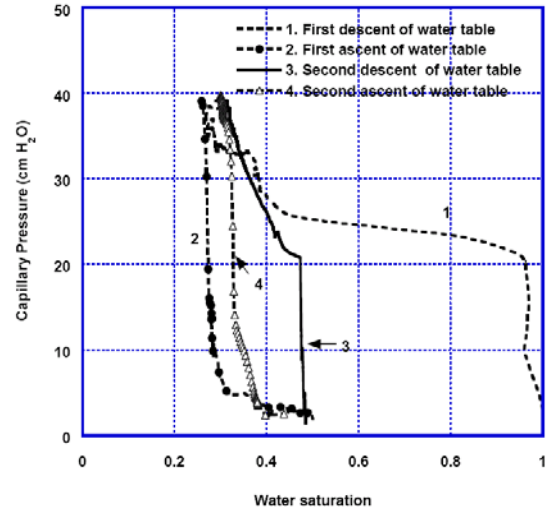

Fig. 5. S-p relation under the influence of water table fluctuation

During the first drainage process, the water saturation decreased from a value of 1.0 to 0.22, during the first imbibition process it increased from 0.22 to 0.5, during the second drainage process it decreased from 0.5 to 0.3, and during the second imbibition process it increased from 0.3 to 0.5. The effect of hysteresis during the whole experiment is evident since the *S-p* relation is history and path dependent.

In order to describe the *S-p* relation under fluctuating water table with a mathematical expression, the VG model was selected to fit the measured data using the modified Gauss-Newton method (Hartley 1961).

A widely accepted empirical parameter form, the VG model by van Genuchten (1980), was rewritten as (Helmig 1997):

$$h_{cij} = \frac{1}{\alpha}\left(S_{je}^{-1/m} - 1\right)^{1/n} \qquad h_{cij} > 0 \tag{1}$$

where h_{cij} (cm) is the capillary pressure head between nonwetting fluid *i* and wetting fluid *j*, α (1/cm) and *n* are parameters, and $m = 1\text{-}1/n$.

The effective saturation of the *j* phase, wetting fluid phase, S_{je} is defined as:

$$S_{je} = \frac{S_w - S_{wr}}{1 - S_{wr} - S_{nr}} \qquad S_{wr} \le S_w \le 1 - S_{nr} \tag{2}$$

where S_{wr} and S_{nr} are irreducible water saturation and residual LNAPL saturation respectively.

To obtain the residual saturation, we may use one of two basic methods: the first one is by extrapolating the measured data, and the second one is by taking it at some arbitrarily large capillary pressure (Corey 1994). Both provide us with theoretical values, and there is no way to obtain the absolute value of this residual saturation via an experimental method.

Some assumptions were made to obtain the parameters of the VG model. Depending on the column test, the first and second descent processes can both be regarded as incomplete drainage processes. Namely, during these two drainage processes, water saturation did not reach its extreme value, i.e., irreducible water saturation. However, during the second ascent process, water saturation could not increase any more after a longer time (97 hours). Thus, with regard to this column test, it will be assumed that the LNAPL saturation reached its extreme value, residual saturation, during the second ascent process of the water table. From the first descent process of water table the value of the irreducible water saturation can be obtained using the modified Gauss-Newton fitting method. From the second ascent process of the water table, the value of reducible LNAPL saturation can also be obtained.

The fitted results are shown in Table 2 and Fig. 6. The coefficients of correlation are high, thus, the fitting

process was successful. It is clear that hysteresis takes a very important effect during the descent and ascent of the water table. The *S-p* relation is absolutely history and path dependent.

Table 2. Fitted parameters of *S-p* model under the influence of fluctuating water table

	α	n	S_{wr}	S_{nr}	R
1st drainage	0.041	6.19	0.17	0	0.95
1st imbibition	13.80	1.21	0.17	0.50	0.97
2nd drainage	0.037	2.80	0.17	0.50	0.98
2nd imbibition	0.73	1.28	0.17	0.50	0.98

R is the coefficient of correlation

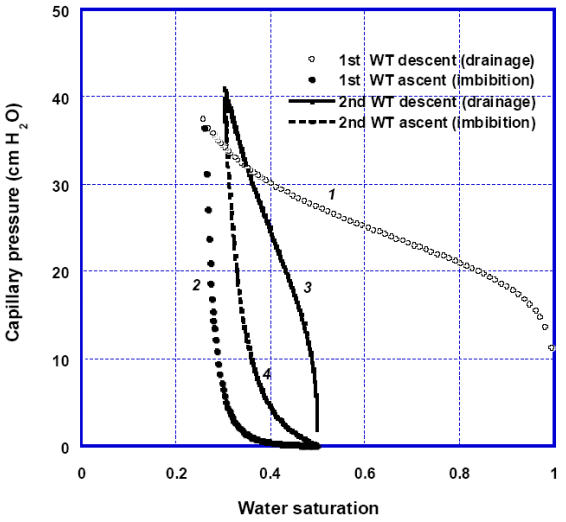

Fig. 6. Fitted *S-p* relation under the influence of water table fluctuation

3. Numerical Analysis

3.1 NAPL Simulator

NAPL Simulator is a complete subsurface flow and transport mathematical model developed by the National Risk Management Research Laboratory of the EPA to study the movement and fate of NAPL contaminants in near-surface granular soils (Guarnaccia et al. 1997). It works with three fundamental and interrelated physical processes: multiphase flow, which defines the time-dependant volumetric extent of the mobile and immobile components of the water, NAPL and gas phases; interphase mass transfer, which defines how the NAPL contaminants partition among phases, i.e., water, NAPL, and gas phases; and constituent mass transport, which defines the temporal and spatial distribution of NAPL contaminants within a given phase.

Particular attention has been paid to quantifying four processes: fluid entrapment and release, hysteresis in the relative permeability–saturation–capillary pressure model, rate–limited mass transfer to describe NAPL dissolution and volatilization, and advective–dispersive transport in both the water and gas phases.

NAPL Simulator uses a set of coupled nonlinear partial differential balance equations (PDE's) to govern the temporal and spatial variability of the system, and a set of constitutive and thermodynamic equations which relate physically-based parameters occurring in the PDE's to the dependent variables.

It focuses on three-phase relative permeability-saturation-capillary pressure relationships which includes flow-path-history-dependent functions (i.e., hysteresis), fluid entrapment considerations, functional dependence on fluid and soil properties; and on rate-limited interphase processes, including NAPL dissolution and volatilization.

3.2 Modification of NAPL Simulator

(1) Effect of Hysteresis on LNAPL Migration in Case of Incomplete Drainage and Imbibition Processes

Fluctuation of the water table can cause drainage and imbibition of a porous medium saturated with LNAPL. In general, this drainage and imbibition processes are somehow incomplete. Thus, for a porous medium initially saturated with water, the *S-p* curves in the case of fluctuating water table can be described as following the sequence PDC(1), SIC(4'), SDC(5) and SIC(4") pictured in Fig. 7.

According to Land (1968) the current trapped gas saturation S_{at} is different at any point of an incomplete *S-p* curve. When an imbibition process begins at the point $S_W = 1 - S_G^{max}$, the resulting residual gas saturation S_{gr}^* is between zero and full residual S_{gr}, which is reasonable from a physics viewpoint. However, if this theory is applied, the simulated trapped LNAPL saturation will result in a much lower value than that of the column test and, therefore, all the simulated results will be completely different from those of the column test. It was found that if the relation $S_{gr}^* = S_{gr}$ is used, the simulated results are close to the column test results. This modification is also appropriate to the general rule of hysteresis (Bear 1972; Helmig 1997; Fetter 1999; Corey 1994).

Some lines were modified on subroutines *hyst_ic.for*

and *trap_up.for* of *NAPL Simulator*'s source file *hyst.f*, in order to use the aforementioned relation $S_{gr}^{*} = S_{gr}$

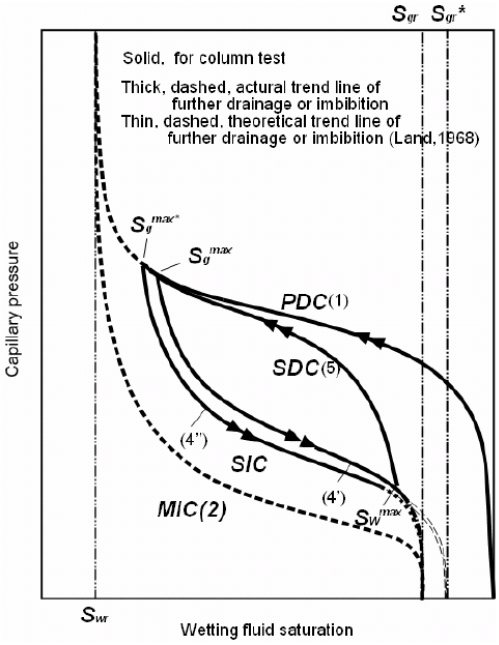

Fig. 7. Difference in residual saturation between complete imbibition and incomplete imbibition processes

(2) Modifications of the source code of NAPL Simulator

Besides the mentioned change, some additional re-encoding had to be done on subroutines *trap_up* and *hyst_ic* due to the modification of hysteresis theory:

(a) In subroutine *dslugm*, an incomplete LU preconditioned GMRES from SLATEC library routine, to add the definition of functions, DMACH and IMACH,

(b) In the same subroutine *dslugm*, to change the dimension of working array, from *iwork (10)*, to *iwork (*)*, otherwise the problem *array bounds exceeded* will be produced during the compilation process. For the working array *iwork* the actual value of array dimension called during simulation is much larger than the defined value.

(c) In the subroutine *exchange*, which computes the mass exchange terms for the water and gas phases, to change the word *bow_2* to *bog_2* in line 290.

3.3 Boundary and initial conditions

As mentioned in 2.3, this column test can be described as having four successive parts:

(a) First descent period, from hour 0 to 89th. The water table is lowered from a height of 45 cm to 5.5 cm above the bottom of the column. The sand is initially fully saturated with water. Then the initially saturated sand is allowed to drain and the pore water was displaced by the LNAPL.

(b) First ascent period, from hour 89th to 150th. The water table is raised to 74.3 cm above the bottom of the column. The initial conditions SW and SN are taken from the last simulated results of the first descent period of water table.

(c) Second descent period, from hour 150th to 216th. The water table was brought down again to 5.5 cm above the column. The initial conditions SW and SN are taken from the last water and LNAPL saturation of the simulated results of the first ascent period of water table.

(d) Second ascent period, from hour 216th hour to 313th. The initial conditions SW and SN are taken from the last water and LNAPL saturation of the simulated results of the second descent period of water table.

The simulation area is 44 cm (length of porous medium) × 3.5 cm (width of porous medium). The two side faces of the column are closed boundaries to any fluid. Only the top and the bottom of the column are open boundaries to water and LNAPL. The discretization of the simulation area for the column test is a 176 isoparametric-element mesh, each element of 1cm × 0.875 cm, making a total of 225 nodes, and it is shown in Fig. 8.

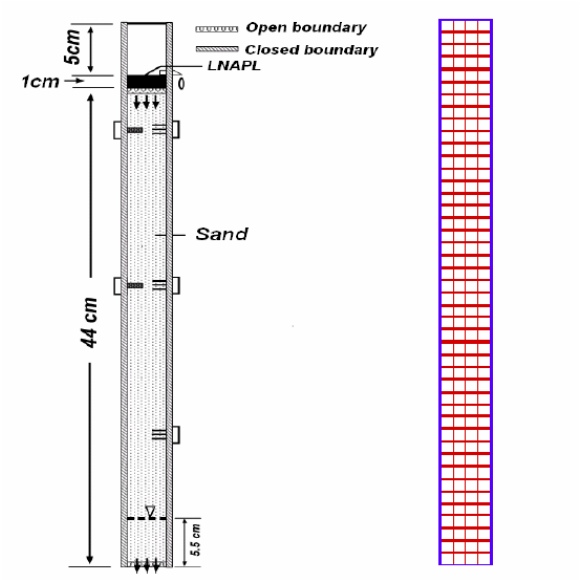

Fig. 8. Boundary conditions and discretization mesh of the column test.

3.4 Results of the column test simulation

Liquid paraffin is insoluble in water and does not vaporize into the air (Table 1), its physicochemical characteristics are very stable under natural conditions and the total simulation time is less than 350 hours. Therefore dissolution, vaporization and degradation of NAPL are all neglected.

From Fig. 9 it is clear that *NAPL Simulator* provides with a very good simulation of the saturation values. However, capillary pressure simulated values (Fig. 10) do not correspond well to measured ones, and this will result in a slightly different simulated versus measured *S-p* relation. The reason may be either the algorithm used to calculate the capillary pressure, or the settled criteria for iteration convergence.

However, as the main goal of NAPL Simulator is to predict NAPL saturation in subsurface, not its capillary pressure, we can conclude that this is a good simulator for our purposes.

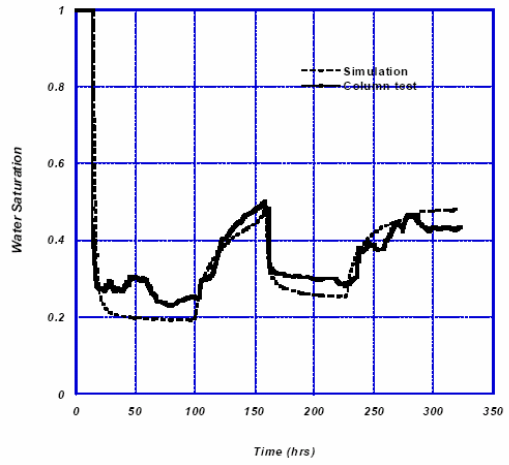

Fig. 9. Simulated and measured saturation

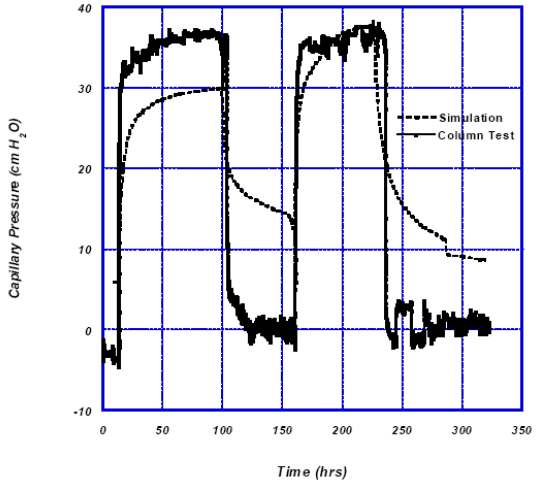

Fig. 10. Simulated and measured capillary pressure

4. Simulation of Benzene Behavior

4.1 Characteristics of Stratum and In-Situ Benzene Contamination

The location of the benzene-contaminated site concerned in this study, as well as the horizontal distribution of benzene concentration (obtained at a depth of 10 m), are shown in Fig. 11. The 30m thick stratum is mainly composed of four layers (from top to bottom): artificial debris layer (very thin), alluvial sand layer (10 m), alluvial sandy clay layer (15 m), and alluvial sand layer (5 m).

From this graphic it is clear that there were two main contamination centers. The higher concentration of benzene appeared at the east part, and the lower concentration appeared at the west part. The flow direction of the groundwater is from east to west. Thus, it can be concluded that the pollution source of benzene might have been in the upstream of the site.

The vertical distribution of the benzene concentration along the section AA' (in the groundwater flow direction) is shown in Fig. 12. We can see some benzene (a LNAPL) located *below* the present water table.

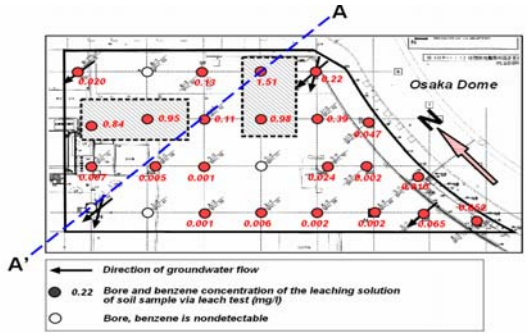

Fig. 11. Horizontal distribution of benzene contamination in the soil at a depth of 10m

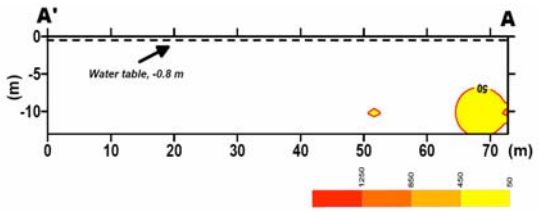

Fig. 12. Vertical distribution of benzene in the AA' section (10^{-3} mg/l)

4.2 Benzene Contamination Origin

In the upstream of the contaminated site, where Osaka Dome is located nowadays, there was a gas plant from 1905 to 1965. The raw material for producing gas

was coal and the production technique from 1905 to 1955 was dry distillation. In reference to the boring core, coal tar appeared in the subsurface and, in both the sand layer and the sandy clay layer, a dark brown liquid, whose appearance is similar to crude oil, also appeared. Thus it could be concluded that the contaminant source of this area might be coal tar, crude oil or a mixture of both.

The changes of groundwater depth monitored in Nishikujo, Osaka (Environmental Protection Bureau of Osaka City, 1995) are shown in Fig. 13. From 1946 to 1962 the water table fell due to groundwater extraction. After that, it ascended yearly until it reached a depth of 0.8 m in 2000. From 1978 to 1999 there is no available information and, therefore, the dashed line is an assumption based on the existing data.

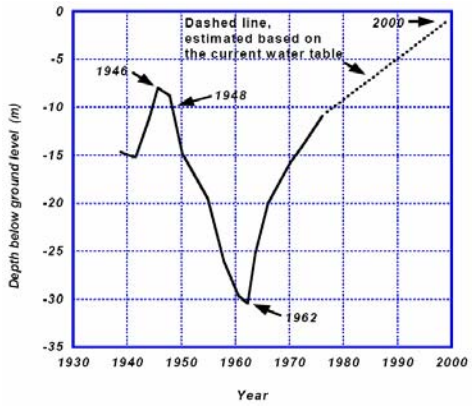

Fig. 13. Water table versus time in Nishikujyo, Osaka

4.3 Simulation with NAPL Simulator

(1) Assumptions made for the in-situ simulation

Both liquid paraffin and benzene are LNAPLs. Liquid paraffin consists mainly of a mixture of saturated straight-chain hydrocarbons. It is a substance that in its pure form is white, odorless and translucent and has the approximate chemical formula of $C_{20}H_{42}$. Benzene is a volatile aromatic hydrocarbon and is known to be a human carcinogen. Thus, liquid paraffin was used as a substitute LNAPL sample in the column test. The main properties of both are shown in Table 3.

Toyoura sand was used in the column test as a substitute for the porous media in the in-situ contaminated subsurface, because of lack of precise information about the grain size distributions of the actual sand layers.

The residual saturation of liquid paraffin measured by the column test was fitted to 0.5. Actually, the residual saturation of benzene in the in-situ contaminated subsurface should not be so large due to its much lower viscosity. Therefore, it will be assumed to be 0.20 in sand layer and 0.25 in sandy clay layer.

Table 3. Properties of Liquid Paraffin and Benzene

	Liquid Paraffin	Benzene
Formula	$C_{20}H_{42}$ (or above)	C_6H_6
Appearance	Colorless, Odorless	Colorless
Boiling Point	> 300°C	80.1°C
Melting Point	< -10°C	5.5°C
Solubility in Air	Non Volatile	161 mg/l
Solubility in H_2O	Insoluble	1780 mg/l (20°C)
Viscosity	170 mpa·s	0.647 mpa·s
Hazard Nature	Non Toxic	Toxic
Surface Tension	31.07 mN/m (25°C)	28.9 mN/m
Interfacial Tension	62.06 mN/m (25°C)	35.0 mN/m
Specific Gravity	0.87 g/cm^3	0.879 g/cm^3

R is the coefficient of correlation

(2) Space discretization and mesh definition

The AA' section shown in Fig. 12 was selected as the section for 2-dimensional simulation. The simulated subsurface is composed from top to bottom of three layers: sand layer, sandy clay layer and sand layer respectively. The discretization of the simulation area (shown in Fig. 14) is a 1500 isoparametric-element mesh, each element of 2m×2m, making a total of 1616 nodes.

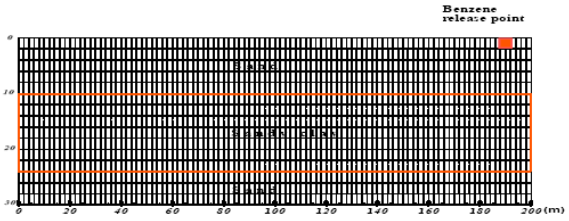

Fig. 14. Space discretization of the simulated subsurface

(3) Analyzed periods

According to data from Fig. 13, three periods were considered:

(a) Benzene infiltration: During this period benzene was released to the subsurface from the top of the subsurface with a head of 20 cm. This contaminant moved with the water flow from right to left following a hydraulic gradient of 0.01.

(b) Descent of water table: During this period, from 1948 to 1963, the water table fell from -10 m to -30 m due to the groundwater extraction. Benzene transported

vertically into the further subsurface with the descent of the water table. Simultaneously, it transported from the right to the left due to the hydraulic gradient of 0.01.

(c) Ascent of water table: During this period, from 1963 to 2001, water table rose gradually from -30 m to -0.8 m. Benzene moved up with the ascent of the water table. Simultaneously it moved from the right to the left due to the hydraulic gradient 0.01.

4.4 Simulation Results

From the simulation described in 4.3, three fundamental mechanisms of benzene migration were found. The first one was its infiltration into the soil and its vertical and lateral migration under the influence of gravitational and capillary forces. The second was the dissolution and consequent advection in the downward-flowing water-phase, or upward-flowing water-phase in the case of seasonal variation of water table. The third was the transport as a vapor benzene constituent in the soil gas, where the increased gas–phase density induced downward movement.

Besides these three migration mechanisms, benzene was also influenced by microorganisms in soil which attenuated, due to decomposition, its presence in subsurface. This influence was taken into account by setting 500 days as the half-life of benzene for the simulation with *NAPL Simulator*.

Figure 15 shows the simulated distribution of benzene one day after the spill. Figure 16 shows the simulated distribution of benzene just after the descent of the water table has finished. Figure 17 shows the simulated distribution of just after the ascent of the water table has finished. It is clear the resemblance among the last one and Fig. 12, which proves that LNAPL can be effectively trapped below the water table if it shows a fluctuating behavior on time.

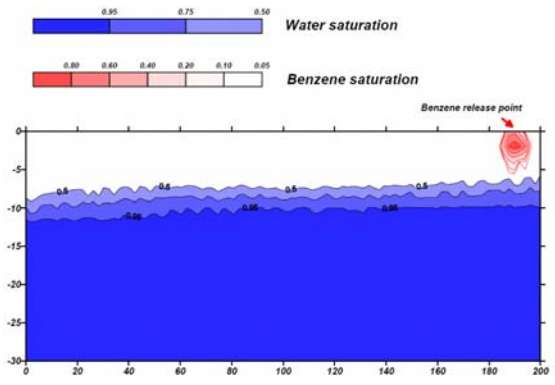

Fig. 15. Distribution of benzene 1 day after the spill

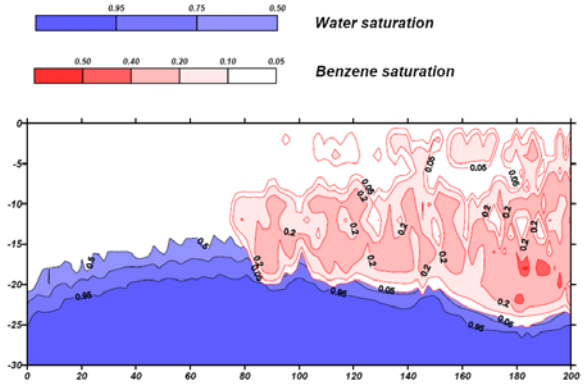

Fig. 16. Distribution of benzene after the descent of the water table has finished

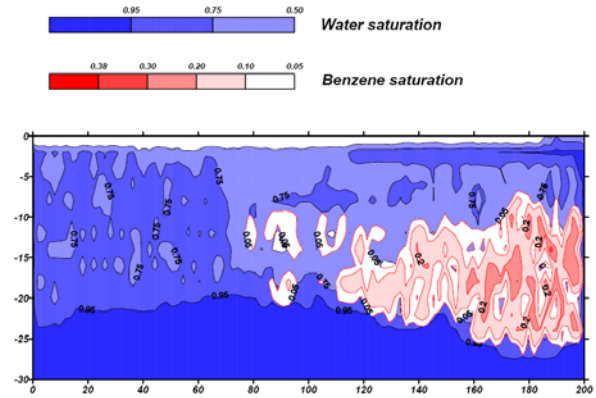

Fig. 17. Distribution of benzene after the ascent of the water table has finished

5. Conclusions

After performing a column test with water table fluctuations, it could be verified that drainage and imbibition are hysteretical processes, since the *S-p* relation is history and path dependent. After some slight modifications, *NAPL Simulator* predicted quite accurately the saturation values of the column test, although the capillary pressure values were not so precise. However, as the main purpose of *NAPL Simulator* is the prediction of NAPL saturation in the subsurface, *NAPL Simulator* has been found as an appropriate model enough to satisfy the purpose.

The simulation using the modified *NAPL Simulator* code was conducted to predict the benzene distribution at a given contaminated location. The predicted results corresponded very well to the in-situ investigated results, demonstrating that the modified *NAPL Simulator* predicts accurately the behavior of benzene under fluctuating water table conditions.

References

Bear, J. (1972): Dynamics of Fluids in Porous Media. Dover Publications, Inc., New York.

Corey, A.T. (1994): Mechanics of Immiscible Fluids in Porous Media. Water Resources Publications.

Endo, K. (2002): Characteristics of DNAPL migration and assessment of DNAPL distribution in a contaminated subsurface, PhD dissertation (in Japanese). Kyoto University, Kyoto, Japan.

Environmental Protection Bureau of Osaka City (1995): White paper on the environment of Osaka.

Fetter, C.W. (1999): Contaminant hydrogeology. Upper Saddle River, New Jersey 07458, Prentice-Hall, Inc., Simon & Schuster/A Viacom Company.

Guarnaccia, J., Pinder, G., and Fishman, M. (1997): NAPL: Simulator Documentation, EPA/600/R-97/ 102. National Risk Management Research Laboratory, United States Environmental Protection Agency, Ada, OK 74820.

Hartley, H. O. (1961): The Modified Gauss-Newton Method for the Fitting of Non-Linear Regression Functions by Least Squares. Technometrics, 3(2), 269-280.

Helmig, R. (1997): Multiphase flow and transport process in the subsurface: A contribution to the modeling of Hydrosystems. Springer.

Kamon, M., Endo, K., and Katsumi, T. (2003): Measuring the *k-S-p* relations on DNAPLs migration. Engineering Geology, 70(3-4), 351-363.

Land, C. S. (1968): Calculation of imbibiiton relative permeability for two-and three-phase flow from rock properties. Trans. Am. Inst. Min. Metall. Pet. Eng.,(243), 149-156.

van Genuchten, M. T. (1980): A Closed-Form Equation for Predicting the Hydraulic Conductivity of Unsaturated Soils. Soil Science Society of America Journal, 44(5), 892-898.

LNAPLの挙動に及ぼす地下水位変動の影響

嘉門雅史[*]・Yan LI[**]・Giancarlo FLORES[***]・乾　徹[*]・勝見　武[*]

[*]京都大学大学院地球環境学堂
[**]中華人民共和国中山大学
[***]京都大学大学院工学研究科

要旨

地下水位が変動する条件下でのベンゼン（LNAPL）の地中での挙動を予測するため、NAPLシミュレーターによる数値解析を行った。NAPLシミュレーターはカラム試験で求めた*S-p*関係を再現できることを示した。さらにNAPLシミュレーターのコードの微修正により、カラム試験で得られた水およびLNAPLの飽和度、流速、液圧を良好に表現できた。この修正コードを用いて、実際の汚染サイトを対象に地下水位が変動する条件でのベンゼンの挙動を解析し、実際の現地調査の結果との比較を行った。解析結果と実測結果は良好な対応を示しており、修正NAPLシミュレーターは地下水位変動条件下でのベンゼンの挙動の評価に用いうることを示した。

キーワード:　地下水，汚染，ベンゼン、LNAPL，カラム試験，*S-p*曲線